

Infrared Spectroscopic and Density Functional Theory Study on the Reactions of Rhodium and Cobalt Atoms with Carbon Dioxide in Rare-Gas Matrixes

Ling Jiang, Yun-Lei Teng, and Qiang Xu*

National Institute of Advanced Industrial Science and Technology (AIST), Ikeda, Osaka 563-8577, Japan, and Graduate School of Science and Technology, Kobe University, Nada Ku, Kobe, Hyogo 657-8501, Japan

Received: April 11, 2007; In Final Form: May 31, 2007

Reactions of laser-ablated rhodium and cobalt atoms with carbon dioxide molecules in solid argon and neon have been investigated using matrix isolation infrared spectroscopy. The OMCO, O₂MCO, OMCO⁻ (M = Rh, Co), OCo₂CO, and OCoCO⁺ molecules have been formed and characterized on the basis of isotopic shifts, mixed isotopic splitting patterns, ultraviolet irradiation, CCl₄-doping experiments, and the change of laser power. Density functional theory calculations have been performed on these products. The overall agreement between the experimental and calculated vibrational frequencies, relative absorption intensities, and isotopic shifts supports the identification of these products from the matrix infrared spectrum.

Introduction

The interaction of metals with carbon dioxide is of considerable interest because of its importance in a great number of catalytic processes.^{1–8} Metal-catalyzed activation of carbon dioxide has many potential incentives with economic and environmental benefits.^{1–8} Extensive efforts have been made to recycle CO₂ from industrial emissions and to remove some of this greenhouse gas.^{1–8} Transition metal catalysts have been widely used in such processes. The dissociation of CO₂ on supported rhodium catalyst has been detected by infrared spectroscopy above 523 K.⁹ Furthermore, the addition of Pt, Pd, or Rh exhibited a significant promotion for the reforming of CH₄ with CO₂ over Ni_{0.03}Mg_{0.970} solid solution catalyst.¹⁰

Reactions of metal atoms with carbon dioxide have been investigated, and a series of metal–carbon dioxide complexes have been experimentally characterized.^{11–31} Quantum chemical calculations have been performed to understand the electronic structures and bonding characteristics of these complexes.^{11–34} The insertion product (OMCO) has been observed for all first-row transition metal atoms except Cu and Zn in rare-gas matrixes.^{15–23} The reactions of Cr through Cu atoms with CO₂ give OMCO⁻ anions, and Co, Ni, and Cu atoms also produce additional MCO₂⁻ anions.^{15–23}

Recent studies have shown that, with the aid of isotopic substitution technique, matrix isolation infrared spectroscopy combined with quantum chemical calculation is very powerful in investigating the spectrum, structure, and bonding of novel species.^{35,36} In contrast to extensive experimental and theoretical studies of the interactions of CO₂ molecules with the transition metal and main group element atoms,^{11–31} however, much less work has been done on the Rh + CO₂ reactions. Recently, argon matrix investigations of the reactions of laser-ablated Co metal atoms with CO₂ molecules have characterized the OCoCO, OCoCO⁻, and CoCO₂⁻ molecules.²³ Here we report a study of reactions of laser-ablated rhodium and cobalt atoms with carbon dioxide in solid argon and neon. IR spectroscopy coupled with theoretical calculations provides evidence for the formation of

the OMCO, O₂MCO, OMCO⁻ (M = Rh, Co), OCo₂CO, and OCoCO⁺ molecules.

Experimental and Theoretical Methods

The experiment for laser ablation and matrix isolation infrared spectroscopy is similar to those previously reported.^{37,38} In short, the Nd:YAG laser fundamental (1064 nm, 10 Hz repetition rate with 10 ns pulse width) was focused on rotating Rh and Co targets. Laser-ablated Rh and Co atoms were codeposited with CO₂ in excess argon (or neon) onto a CsI window cooled normally to 4 K by means of a closed-cycle helium refrigerator. Typically, 1–20 mJ/pulse laser power was used. CO₂ (99.99%, Takachiho Chemical Industrial Co., Ltd.), ¹³C¹⁶O₂ (99%, ¹⁸O < 1%, Cambridge Isotopic Laboratories), ¹²C¹⁸O₂ (95%, Cambridge Isotopic Laboratories), ¹²C¹⁶O₂ + ¹³C¹⁶O₂, and ¹²C¹⁶O₂ + ¹²C¹⁸O₂ were used in different experiments. In general, matrix samples were deposited for 30–60 min with a typical rate of 2–4 mmol/h. After sample deposition, IR spectra were recorded on a Bio-Rad FTS-6000e spectrometer at 0.5 cm⁻¹ resolution using a liquid nitrogen cooled HgCdTe (MCT) detector for the spectral range of 5000–400 cm⁻¹. Samples were annealed at different temperatures and subjected to broad-band irradiation for 10–15 min using a high-pressure mercury arc lamp (Ushio, 100 W, λ > 250 nm).

Density functional theory (DFT) calculations were performed to predict the structures and vibrational frequencies of the observed reaction products using the Gaussian 03 program.³⁹ The BP86 density functional method was used.⁴⁰ The 6-311+G(d) basis set was used for the C and O atoms,⁴¹ and the Los Alamos ECP plus DZ (LANL2DZ) basis set was for the Rh and Co atoms.⁴² Geometries were fully optimized, and vibrational frequencies were calculated with analytical second derivatives. Previous investigations have shown that such computational methods can provide reliable information for metal complexes, such as infrared frequencies, relative absorption intensities, and isotopic shifts.^{11–38}

Results and Discussion

Experiments have been done with carbon dioxide concentrations ranging from 0.02% to 2.0% in excess argon and neon.

* Corresponding author. E-mail: q.xu@aist.go.jp.

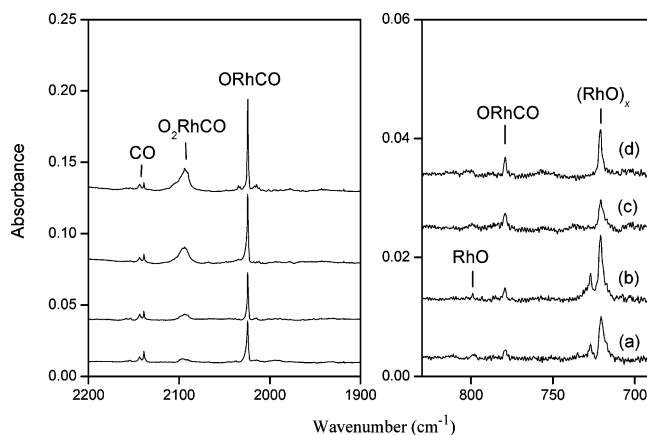


Figure 1. Infrared spectra in the 2200–1900 and 800–700 cm^{-1} regions from codeposition of laser-ablated Rh atoms with 1.0% CO_2 in Ar. (a) After 1 h of sample deposition at 4 K, (b) after annealing to 25 K, (c) after 10 min of broad-band irradiation, and (d) after annealing to 30 K.

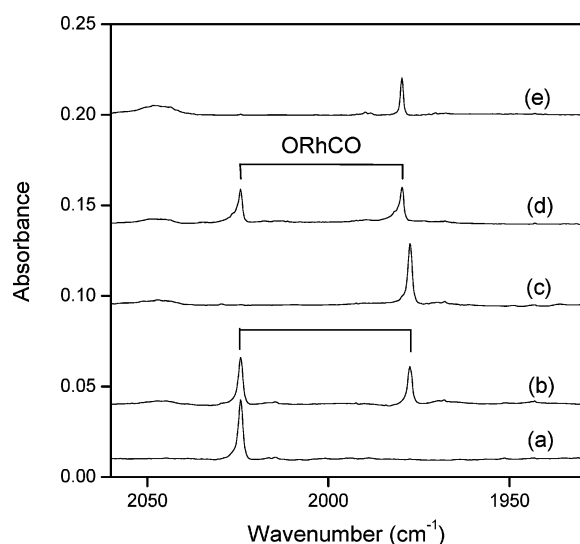


Figure 2. Infrared spectra in the 2050–1950 cm^{-1} region for laser-ablated Rh atoms codeposited with isotopic CO_2 in Ar after annealing to 25 K. (a) 1.0% $^{12}\text{C}^{16}\text{O}_2$, (b) 0.7% $^{12}\text{C}^{16}\text{O}_2$ + 0.7% $^{13}\text{C}^{16}\text{O}_2$, (c) 1.0% $^{13}\text{C}^{16}\text{O}_2$, (d) 0.7% $^{12}\text{C}^{16}\text{O}_2$ + 0.7% $^{12}\text{C}^{18}\text{O}_2$, and (e) 1.0% $^{12}\text{C}^{18}\text{O}_2$.

The experiments of the Co atoms with CO_2 in the argon matrix have been reported previously²³ and will not be shown in the present study. Typical infrared spectra for the reactions of laser-ablated Rh atoms with CO_2 molecules in excess argon and neon in the selected regions are illustrated in Figures 1–4, and those for the reactions of laser-ablated Co atoms with CO_2 molecules in excess neon in the selected regions are illustrated in Figures 5–7. The absorption bands in different isotopic experiments are listed in Tables 1 and 2. The stepwise annealing and irradiation behavior of the product absorptions is also shown in the figures and will be discussed below. Experiments were also done with different concentrations of CCl_4 serving as an electron scavenger. The absorptions of the RhO , $(\text{RhO})_x$,⁴³ CoO ,⁴⁴ CO , CO_4^- , and C_2O_4^- ^{45–49} molecules have also been observed in the present experiments and will not be discussed here. It is noted that the $(\text{RhO})_x$ absorptions increase sharply and new absorptions increase slightly with the increase of the laser power in the $\text{Rh} + \text{CO}_2$ reaction, suggesting that these new absorptions involve one Rh atom other than Rh_x .

Quantum chemical calculations have been carried out for the possible isomers and electronic states of the potential product molecules. Figure 8 shows the optimized structures of the

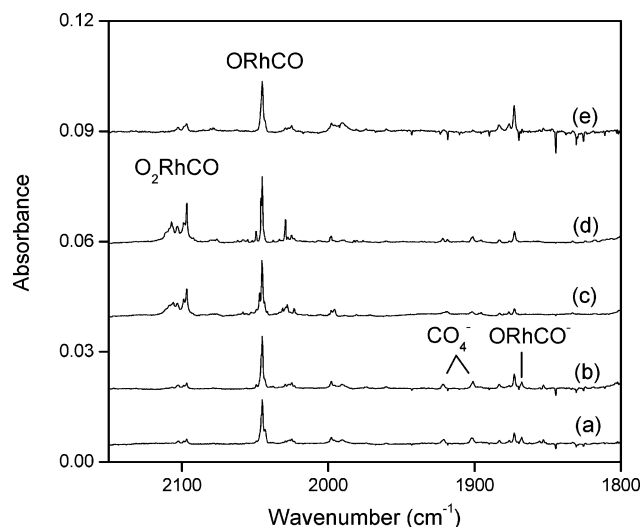


Figure 3. Infrared spectra in the 2150–1800 cm^{-1} region from codeposition of laser-ablated Rh atoms with 0.3% CO_2 in Ne. (a) After 45 min of sample deposition at 4 K, (b) after annealing to 10 K, (c) after 12 min of broad-band irradiation, (d) after annealing to 12 K, and (e) 0.3% CO_2 + 0.05% CCl_4 , after annealing to 10 K.

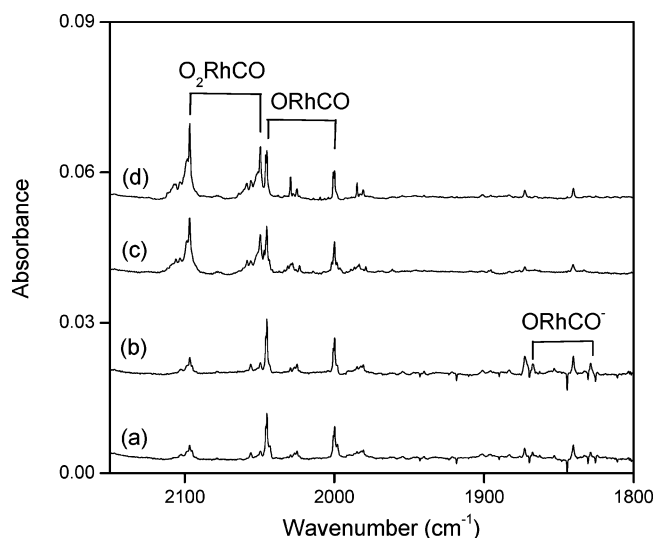


Figure 4. Infrared spectra in the 2150–1800 cm^{-1} region from codeposition of laser-ablated Rh atoms with 0.2% $^{12}\text{C}^{16}\text{O}_2$ + 0.2% $^{12}\text{C}^{18}\text{O}_2$ in Ne. (a) After 45 min of sample deposition at 4 K, (b) after annealing to 10 K, (c) after 12 min of broad-band irradiation, and (d) after annealing to 12 K.

possible reaction products. The comparison of the observed and calculated isotopic frequency ratios for the C–O and M–O ($M = \text{Rh}, \text{Co}$) stretching modes of the products is summarized in Table 3. The ground electronic states, point groups, vibrational frequencies, and intensities are listed in Table 4.

ORhCO. In the reaction of the Rh atoms with CO_2 in the argon matrix, two absorptions at 2024.2 and 779.2 cm^{-1} appear together during sample deposition, change little after annealing to 25 K, increase visibly after broad-band irradiation, and increase slightly after further annealing to higher temperature (Table 1 and Figure 1). The upper band at 2024.2 cm^{-1} shifts to 1977.4 cm^{-1} with $^{13}\text{C}^{16}\text{O}_2$ and to 1979.7 cm^{-1} with $^{12}\text{C}^{18}\text{O}_2$, exhibiting isotopic frequency ratios ($^{12}\text{C}^{16}\text{O}_2/^{13}\text{C}^{16}\text{O}_2$, 1.0237; $^{12}\text{C}^{16}\text{O}_2/^{12}\text{C}^{18}\text{O}_2$, 1.0225) characteristic of C–O stretching vibrations. The mixed $^{12}\text{C}^{16}\text{O}_2 + ^{13}\text{C}^{16}\text{O}_2$ and $^{12}\text{C}^{16}\text{O}_2 + ^{12}\text{C}^{18}\text{O}_2$ isotopic spectra (Figure 2) only provide the sum of pure isotopic bands, which indicates only one CO unit is involved in this carbonyl stretching mode.⁵⁰ The 779.2 cm^{-1} band shows no

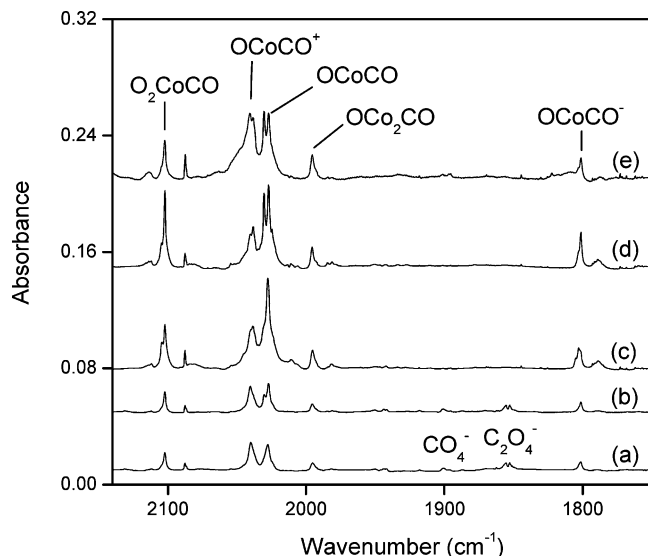


Figure 5. Infrared spectra in the 2100–1800 cm⁻¹ region from codeposition of laser-ablated Co atoms with 0.4% CO₂ in Ne. (a) After 45 min of sample deposition at 4 K, (b) after annealing to 10 K, (c) after 12 min of broad-band irradiation, (d) after annealing to 11 K, and (e) 0.3% CO₂ + 0.05% CCl₄, after 12 min of broad-band irradiation and annealing to 11 K.

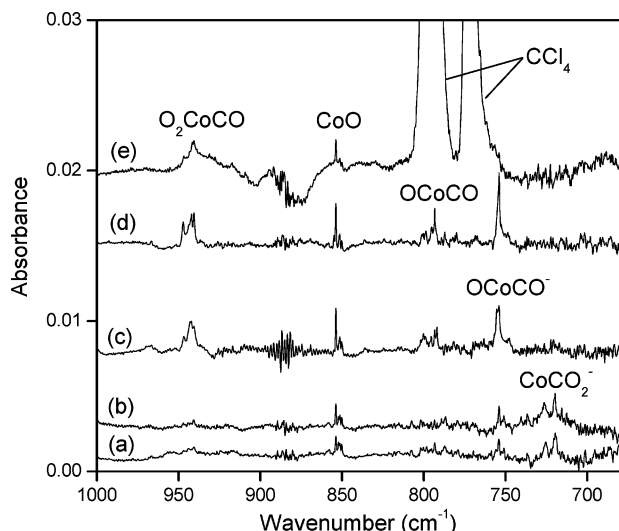


Figure 6. Infrared spectra in the 1000–700 cm⁻¹ region from codeposition of laser-ablated Co atoms with 0.4% CO₂ in Ne. (a) After 45 min of sample deposition at 4 K, (b) after annealing to 10 K, (c) after 12 min of broad-band irradiation, (d) after annealing to 11 K, and (e) 0.3% CO₂ + 0.05% CCl₄, after 12 min of broad-band irradiation and annealing to 11 K.

carbon isotopic shift, but shifts to 740.1 cm⁻¹ with ¹²C¹⁸O₂. The ¹²C¹⁶O₂/¹²C¹⁸O₂ isotopic frequency ratio of 1.0528 is very close to the diatomic Rh¹⁶O/Rh¹⁸O frequency ratio of 1.0516,⁴³ suggesting a Rh–O stretching mode. Only doublets have been observed in the ¹²C¹⁶O₂ + ¹²C¹⁸O₂ isotopic spectra. Furthermore, doping with CCl₄ has no effect on these bands (not shown here), suggesting that the product is neutral.⁵¹ The 2024.2 and 779.2 cm⁻¹ bands are therefore assigned to the C–O and Rh–O stretching vibrations of the neutral ORhCO molecule, respectively. The corresponding C–O and Rh–O stretching frequencies of ORhCO in solid neon appear at 2045.0 and 790.1 cm⁻¹ (Table 1 and Figure 3), respectively, which are 20.8 and 10.9 cm⁻¹ blue-shifted from the argon matrix counterpart.

BP86 calculations predict that the ORhCO molecule has a C_s symmetry with a ²A'' ground state (Table 4 and Figure 8),

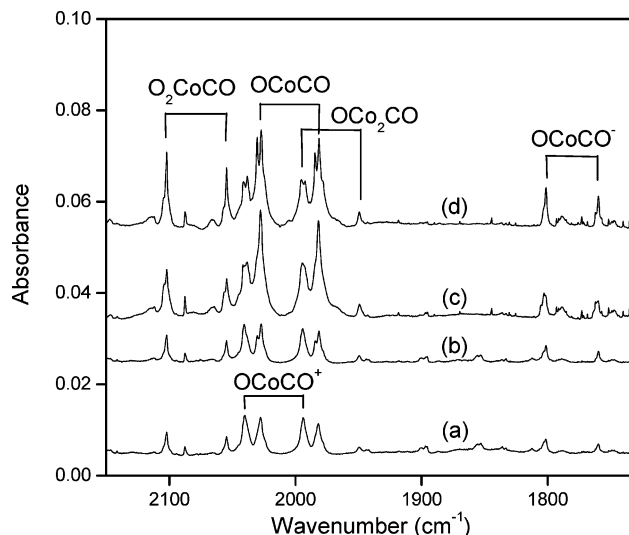


Figure 7. Infrared spectra in the 2100–1800 cm⁻¹ region from codeposition of laser-ablated Co atoms with 0.3% ¹²C¹⁶O₂ + 0.3% ¹³C¹⁶O₂ in Ne. (a) After 45 min of sample deposition at 4 K, (b) after annealing to 10 K, (c) after 12 min of broad-band irradiation, and (d) after annealing to 11 K.

which lies 4 kcal/mol lower in energy than a ⁴A' one. For the C–O stretching mode, the vibrational frequency is calculated to be 2019.7 cm⁻¹ with the ¹²C¹⁶O₂/¹³C¹⁶O₂ and ¹²C¹⁶O₂/¹²C¹⁸O₂ isotopic frequency ratios of 1.0245 and 1.0221 (Tables 3 and 4), respectively, which are in agreement with the experimental observations. The Rh–O stretching vibration is predicted to be 776.3 cm⁻¹, and the calculated ¹²C¹⁶O₂/¹²C¹⁸O₂ isotopic frequency ratio of 1.0526 is consistent with the experimental value of 1.0528 (Table 3). These agreements support the assignment of the ORhCO molecule.

O₂RhCO. In the reaction of the Rh atoms with CO₂ in the neon matrix, the absorption at 2096.7 cm⁻¹ appears weakly during sample deposition, changes little after annealing to 10 K, increases sharply after broad-band irradiation, and increases slightly after further annealing to 12 K (Table 1 and Figure 3). This band shifts to 2049.2 cm⁻¹ with ¹³C¹⁶O₂ and to 2049.4 cm⁻¹ with ¹²C¹⁸O₂, exhibiting isotopic frequency ratios (¹²C¹⁶O₂/¹³C¹⁶O₂, 1.0232; ¹²C¹⁶O₂/¹²C¹⁸O₂, 1.0231) characteristic of C–O stretching vibrations. The mixed ¹²C¹⁶O₂ + ¹²C¹⁸O₂ isotopic spectra (Figure 4) only provide the sum of pure isotopic bands, which indicates that only one CO unit is involved in this carbonyl stretching mode.⁵⁰

DFT calculations for the O₂RhCO molecule provide the C–O stretching vibrational frequency at 2073.0 cm⁻¹ (583 km/mol) with calculated ¹²C¹⁶O₂/¹³C¹⁶O₂ and ¹²C¹⁶O₂/¹²C¹⁸O₂ ratios in accord with the experimental values (Tables 1, 3, and 4). The antisymmetric O–Rh–O stretching vibrational frequency is calculated at 847.3 cm⁻¹, which has a relatively small intensity (123 km/mol) and is not readily observed, consistent with the absence from the present experiments. The corresponding C–O stretching frequency of the O₂RhCO molecule in solid argon appears at 2093.8 cm⁻¹ (Table 1 and Figure 1).

ORhCO⁻. In the reaction of Rh atoms with CO₂ in the neon matrix, the absorption at 1867.8 cm⁻¹ appears weakly during sample deposition, changes little after annealing to 10 K, disappears after broad-band irradiation, and does not return after further annealing to 12 K (Table 1 and Figure 3). This band shifts to 1823.8 cm⁻¹ with ¹³C¹⁶O₂ and to 1828.9 cm⁻¹ with ¹²C¹⁸O₂, exhibiting isotopic frequency ratios (¹²C¹⁶O₂/¹³C¹⁶O₂, 1.0241; ¹²C¹⁶O₂/¹²C¹⁸O₂, 1.0213) characteristic of C–O stretching vibrations. The mixed ¹²C¹⁶O₂ + ¹²C¹⁸O₂ isotopic spectra

TABLE 1: IR Absorptions (in cm^{-1}) Observed from Codeposition of Laser-Ablated Rh Atoms with CO_2 in Excess Argon and Neon at 4 K

$^{12}\text{C}^{16}\text{O}_2$	$^{13}\text{C}^{16}\text{O}_2$	$^{12}\text{C}^{18}\text{O}_2$	$R(12/13)$	$R(16/18)$	assignment
Ar					
2093.8	2043.1	2043.2	1.0248	1.0248	O_2RhCO
2024.2	1977.4	1979.7	1.0237	1.0225	ORhCO
799.0	799.0	759.8	1.0000	1.0516	RhO
779.2	779.2	740.1	1.0000	1.0528	ORhCO
720.9	720.9	686.2	1.0000	1.0506	$(\text{RhO})_x$
Ne					
2096.7	2049.2	2049.4	1.0232	1.0231	O_2RhCO
2045.0	1998.6	1999.8	1.0232	1.0226	ORhCO
1872.8	1833.0	1840.3	1.0217	1.0177	?
1867.8	1823.8	1828.9	1.0241	1.0213	ORhCO^-
819.9	819.9	781.3	1.0000	1.0494	RhO
790.1	790.1	750.3	1.0000	1.0530	ORhCO

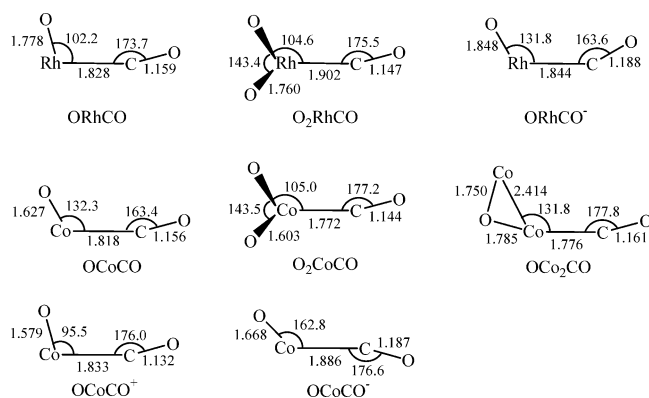
TABLE 2: IR Absorptions (in cm^{-1}) Observed from Codeposition of Laser-Ablated Co Atoms with CO_2 in Excess Neon at 4 K

$^{12}\text{C}^{16}\text{O}_2$	$^{13}\text{C}^{16}\text{O}_2$	$^{12}\text{C}^{18}\text{O}_2$	$R(12/13)$	$R(16/18)$	assignment
2102.2	2054.6	2054.5	1.0232	1.0232	O_2CoCO
2040.4	1994.7	1993.5	1.0229	1.0235	OCoCO^+
2027.1	1981.2	1981.2	1.0232	1.0232	OCoCO
1995.7	1949.2	1951.9	1.0239	1.0224	OC_2CO
1801.3	1759.4	1758.5	1.0238	1.0243	OC_2CO^-
942.9	942.9	905.6	1.0000	1.0412	O_2CoCO
853.7	853.7	816.1	1.0000	1.0461	CoO
793.3	793.3	758.2	1.0000	1.0463	OC_2CO
753.9	753.9	720.9	1.0000	1.0458	OC_2CO^-

TABLE 3: Comparison of Observed (in Neon) and Calculated IR Frequency Ratios for the Products

species	vibrational mode	$R(12/13)$		$R(16/18)$	
		obsd	calcd	obsd	calcd
ORhCO	$\nu_{\text{C-O}}$	1.0232	1.0245	1.0226	1.0221
	$\nu_{\text{Rh-O}}$	1.0000	1.0004	1.0528	1.0526
O_2RhCO	$\nu_{\text{C-O}}$	1.0232	1.0239	1.0231	1.0230
ORhCO^-	$\nu_{\text{C-O}}$	1.0241	1.0247	1.0213	1.0217
OC_2CO	$\nu_{\text{C-O}}$	1.0232	1.0238	1.0232	1.0233
	$\nu_{\text{Co-O}}$	1.0000	1.0000	1.0463	1.0460
O_2CoCO	$\nu_{\text{C-O}}$	1.0232	1.0240	1.0232	1.0228
	$\nu_{\text{Co-O}}$	1.0000	1.0001	1.0412	1.0404
OC_2CO	$\nu_{\text{C-O}}$	1.0239	1.0241	1.0224	1.0227
OC_2CO^-	$\nu_{\text{C-O}}$	1.0238	1.0248	1.0243	1.0217
	$\nu_{\text{Co-O}}$	1.0000	1.0000	1.0458	1.0451
OC_2CO^+	$\nu_{\text{C-O}}$	1.0229	1.0235	1.0235	1.0235

(Figure 4) only provide the sum of pure isotopic bands, which indicates only one CO unit is involved in this carbonyl stretching mode.⁵⁰ Furthermore, the 1867.8 cm^{-1} band disappears after doping with CCl_4 (Figure 3, trace e), suggesting that the product is anionic.⁵¹ Accordingly, the 1867.8 cm^{-1} band is assigned to the C–O stretching vibration of the ORhCO^- anion. The argon

**Figure 8.** Optimized structures (bond lengths in angstroms, bond angles in degrees) of possible reaction products.

counterpart of ORhCO^- is absent from the present matrix experiments.

The present DFT calculations predict that the ORhCO^- molecule has a $^3A''$ ground state with a C_s symmetry (Table 4 and Figure 8). The C–O stretching vibrational frequency is calculated at 1842.9 cm^{-1} (1087 km/mol) (Table 4), which is in agreement with the experimental value of 1867.8 cm^{-1} (Table 1). The Rh–O stretching vibration is predicted to be 671.6 cm^{-1} , which has a relatively small intensity (77 km/mol) and is not readily observed, consistent with the absence from the present experiments. The $\angle\text{RhCO}$ angle in the anionic ORhCO^- molecule (163.6°) is slightly smaller than in the neutral ORhCO molecule (173.7°) (Figure 8).

Other Absorption from the Rh + CO_2 Reaction. In the Rh + CO_2 reaction in solid neon (Figure 3), a weak absorption at 1872.8 cm^{-1} appears during sample deposition, increases slightly after annealing to 10 K, decreases markedly after broadband irradiation, and recovers slightly after further annealing. This band shifts to 1833.0 cm^{-1} with $^{13}\text{C}^{16}\text{O}_2$ and to 1840.3 cm^{-1} with $^{12}\text{C}^{18}\text{O}_2$, giving $^{12}\text{C}^{16}\text{O}_2/^{13}\text{C}^{16}\text{O}_2$ and $^{12}\text{C}^{16}\text{O}_2/^{12}\text{C}^{18}\text{O}_2$ isotopic frequency ratios of 1.0217 and 1.0177, which suggests that this mode is not a pure C–O stretch mode. Tentatively,

TABLE 4: Ground Electronic States, Point Groups, Vibrational Frequencies (cm⁻¹), and Intensities (km/mol) Calculated for the Reaction Products^a

species	electronic state	point group	frequency (intensity, mode)
ORhCO	² A''	C _s	2019.7 (663, A'), 776.3 (32, A'), 525.6 (9, A'), 428.0 (4, A')
O ₂ RhCO	² A''	C _s	2073.0 (583, A'), 847.3 (123, A''), 806.1 (6, A'), 463.5 (9, A')
ORhCO ⁻	³ A''	C _s	1842.9 (1087, A'), 671.6 (77, A'), 526.0 (3, A'), 421.3 (0.2, A')
OCoCO	⁴ A''	C _s	2025.2 (714, A'), 839.0 (46, A'), 474.7 (16, A')
O ₂ CoCO	² A''	C _s	2108.5 (498, A'), 950.8 (114, A''), 859.9 (3, A'), 511.9 (10, A'), 415.4 (1, A')
OC ₂ CO	³ A'	C _s	1992.3 (1252, A'), 662.0 (21, A'), 544.4 (2, A'), 471.2 (48, A'), 449.7 (9, A'), 444.5 (3, A')
OC ₂ CO ⁻	³ A''	C _s	1839.0 (1177, A'), 781.2 (117, A')
OC ₂ CO ⁺	³ A''	C _s	2186.8 (191, A'), 891.1 (16, A'), 424.2 (4, A')

^a Only the frequencies above 400 cm⁻¹ are listed.

the band at 1872.8 cm⁻¹ is assigned to the absorption of some impurities.

OC₂CO, OCoCO⁻, and CoCO₂⁻. The neon matrix absorptions at 2027.1 and 793.3 cm⁻¹ (Table 2 and Figures 5 and 6) are due to the C–O and Co–O stretching vibrations of the OCoCO molecule, respectively, which are consistent with the previous reports of 2026.6 and 783.8 cm⁻¹ absorptions in argon.²³ The 1801.3 and 753.9 cm⁻¹ bands are due to the C–O and Co–O stretching vibrations of the OCoCO⁻ anion, respectively. Weak absorptions at 1714.9, 1237.3, and 725.4 cm⁻¹ are due to the antisymmetric C–O, symmetric C–O, and Co–C stretching vibrations of the CoCO₂⁻ anion, respectively. Discussions about the OCoCO, OCoCO⁻, and CoCO₂⁻ molecules in solid argon have been reported previously,²³ and we will focus on the new products from the reaction of the Co atoms with CO₂ in the neon matrix in this study.

O₂CoCO. In the reaction of the Co atoms with CO₂ in the neon matrix, the absorptions at 2102.2 and 942.9 cm⁻¹ appear together during sample deposition, change little after annealing to 10 K, increase visibly after broad-band irradiation, and increase markedly after further annealing to higher temperature (Table 2 and Figures 5 and 6). The 2102.2 cm⁻¹ band shifts to 2054.6 cm⁻¹ with ¹³C¹⁶O₂ and to 2054.5 cm⁻¹ with ¹²C¹⁸O₂, exhibiting isotopic frequency ratios (¹²C¹⁶O₂/¹³C¹⁶O₂, 1.0232; ¹²C¹⁶O₂/¹²C¹⁸O₂, 1.0232) characteristic of C–O stretching vibrations. The mixed ¹²C¹⁶O₂ + ¹³C¹⁶O₂ isotopic spectra (Figure 7) only provide the sum of pure isotopic bands, which indicates only one CO unit is involved in this carbonyl stretching mode.⁵⁰ The 942.9 cm⁻¹ band shows no carbon isotopic shift, but shifts to 905.6 cm⁻¹ with ¹²C¹⁸O₂. The ¹²C¹⁶O₂/¹²C¹⁸O₂ isotopic frequency ratio of 1.0412 is lower than the CoO diatomic harmonic ratio of 1.0465 (in argon),⁴⁴ but is much closer to the Co¹⁶O/Co¹⁸O ratio for the ν₃ mode of the OCoO molecule (1.0376, in argon).⁴⁴ A triplet isotopic pattern has been observed in the ¹²C¹⁶O₂ + ¹²C¹⁸O₂ isotopic spectra, suggesting that an antisymmetric O–Co–O stretching mode is involved in this product. Accordingly, the 2102.2 and 942.9 cm⁻¹ bands are assigned to the C–O stretching and antisymmetric O–Co–O stretching vibrations of the O₂CoCO molecule, respectively. The argon counterpart of O₂CoCO is absent from the matrix experiments.²³

BP86 calculations predict that the O₂CoCO molecule has a C_s symmetry with a ²A'' ground state (Table 4 and Figure 8). The C–O stretching and antisymmetric O–Co–O stretching vibrational frequencies are calculated to be 2108.5 (498) and 950.8 cm⁻¹ (114 km/mol) (Table 4), respectively, which are consistent with the experimental observations. A similar agreement has also been obtained for the ¹²C¹⁶O₂/¹³C¹⁶O₂ and ¹²C¹⁶O₂/¹²C¹⁸O₂ isotopic frequency ratios (Table 3).

OC₂CO. In the reaction of the Co atoms with CO₂ in solid neon, the absorption at 1995.7 cm⁻¹ appears weakly during sample deposition, changes little after annealing to 10 K,

increases visibly after broad-band irradiation, and changes little after further annealing to 11 K (Table 2 and Figure 5). This band shifts to 1949.2 cm⁻¹ with ¹³C¹⁶O₂ and to 1951.9 cm⁻¹ with ¹²C¹⁸O₂, exhibiting isotopic frequency ratios (¹²C¹⁶O₂/¹³C¹⁶O₂, 1.0239; ¹²C¹⁶O₂/¹²C¹⁸O₂, 1.0224) characteristic of C–O stretching vibrations. The mixed ¹²C¹⁶O₂ + ¹³C¹⁶O₂ isotopic spectra (Figure 7) only provide the sum of pure isotopic bands, which indicates that only one CO unit is involved in this carbonyl stretching mode.⁵⁰ It is noted that the 1995.7 cm⁻¹ band is favored under the experimental conditions of higher laser energy, indicating that this new absorption should involve more than one Co atom. Doping with CCl₄ has no effect on this band (Figure 5e), suggesting that the product is neutral.⁵¹

BP86 calculations for the OC₂CO molecule provide the C–O stretching vibrational frequency at 1992.3 cm⁻¹ (Table 4 and Figure 8), which is in good agreement with the experimental value of 1995.7 cm⁻¹ (Table 1). The calculated ¹²C¹⁶O₂/¹³C¹⁶O₂ and ¹²C¹⁶O₂/¹²C¹⁸O₂ isotopic frequency ratios of 1.0241 and 1.0227 are consistent with the experimental values of 1.0239 and 1.0224, respectively (Table 3), which suggests the assignment of the OC₂CO molecule. As listed in Table 4, the Co–O and Co–C stretching vibrational frequencies of the OC₂CO molecule are predicted to have relatively small intensities and are not readily observed, in accord with the absence from the present experiments. The argon counterpart of OC₂CO is absent from the matrix experiments.²³ In contrast, the C–O stretching vibrational frequency of the Co₂CO molecule has been observed at 1953.3 cm⁻¹ from the reactions of laser-ablated Co atoms with CO molecules in solid argon.⁵²

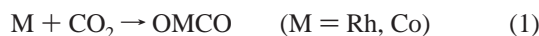
OC₂CO⁺. In the reaction of Co atoms with CO₂ in solid neon, a sharp band at 2040.4 cm⁻¹ appears during sample deposition, and changes little after annealing to 10 K, after broad-band irradiation, and after further annealing to 11 K (Table 2 and Figure 5). This band shifts to 1994.7 cm⁻¹ with ¹³C¹⁶O₂ and to 1993.5 cm⁻¹ with ¹²C¹⁸O₂, exhibiting isotopic frequency ratios (¹²C¹⁶O₂/¹³C¹⁶O₂, 1.0229; ¹²C¹⁶O₂/¹²C¹⁸O₂, 1.0235) characteristic of C–O stretching vibrations. The mixed ¹²C¹⁶O₂ + ¹³C¹⁶O₂ isotopic spectra (Figure 7) only provide the sum of pure isotopic bands, which indicates only one CO unit is involved in this carbonyl stretching mode.⁵⁰ Furthermore, the 2040.4 cm⁻¹ band increases markedly after doping with CCl₄ (Figure 5e), suggesting that the product is cationic.⁵¹ Therefore the cation with the OCoCO⁺ stoichiometry is considered.

DFT calculations predict the C–O stretching vibrational frequencies of the OCoCO⁺, CoOCO⁺, and OCoOC⁺ molecules to be 2186.8, 2404.7, and 1958.7 cm⁻¹, respectively. The OCoCO⁺ and OCoOC⁺ molecules lie 57 and 89 kcal/mol higher in energy than the CoOCO⁺ molecule. However, the calculated C–O stretching vibrational frequency in the CoOCO⁺ molecule (2404.7 cm⁻¹) is much higher than the experimental value of 2040.4 cm⁻¹. Accordingly, the 2040.4 cm⁻¹ band is assigned to the C–O stretching vibration of the OCoCO⁺ cation. As listed

in Table 3, the calculated $^{12}\text{C}^{16}\text{O}_2/^{13}\text{C}^{16}\text{O}_2$ and $^{12}\text{C}^{16}\text{O}_2/^{12}\text{C}^{18}\text{O}_2$ isotopic frequency ratios of 1.0235 and 1.0235 are consistent with the experimental values of 1.0229 and 1.0235, respectively. The Co–O stretching vibration is predicted to be 891.1 cm^{-1} (Table 4), which has relatively small intensity (16 km/mol) and is not readily observed, consistent with the absence from the present experiments.

Reaction Mechanism

On the basis of the behavior of sample annealing and irradiation, together with the observed species and calculated stable isomers, a plausible reaction mechanism can be proposed as follows. Under the present experimental conditions, the OMCO (M = Rh, Co) molecules are the primary products during sample deposition (Figures 1, 3, and 5), suggesting that the spontaneous insertion of laser-ablated Rh and Co atoms into CO_2 to form the OMCO molecules is the dominant process (reaction 1). Similar findings have also been found for the groups 3–10 transition metal atoms.^{15–23} Theoretical investigations reveal that the insertion of metal atoms into CO_2 to form the OMCO molecules needs a low or no energy barrier:^{15–23,32,53}



The observation of RhO, $(\text{RhO})_x$, CoO, and CO shows the presence of the O atoms and the CO molecules. The decomposition of the OMCO molecule may proceed by radiation during sample deposition (reaction 2). The O_2MCO molecule may be formed from the reaction of the OMCO molecule with the O atom (reaction 3) or with another CO_2 molecule (reactions 4 and 5). Under the experimental conditions of higher laser energy, the OC_2CO molecule is generated by the addition of the Co atom to the OC_2CO molecule (reaction 6):



Recent investigations have shown that laser ablation of metal targets produces not only neutral metal atoms, but also metal cations and electrons, and ionic metal complexes can also be formed in the reactions with small molecules.⁵¹ In the present experiments, the OMCO^- anion appears during sample deposition and changes little after sample annealing (Figure 3), suggesting that this anion may be generated by electron capture by neutral OMCO during codeposition (reaction 7). In addition, the OC_2CO^+ molecule may be formed from the reaction of the Co^+ cation with CO_2 (reaction 8):



Conclusions

Reactions of laser-ablated Rh and Co atoms with CO_2 molecules in solid argon and neon have been investigated using matrix isolation infrared spectroscopy. On the basis of isotopic shifts, mixed isotopic splitting patterns, ultraviolet irradiation, and CCl_4 -doping experiments, absorptions at 2024.2 and 779.2

cm^{-1} in argon and 2045.0 and 790.1 cm^{-1} in neon are assigned to the C–O and Rh–O stretching vibrations of the ORhCO molecule, respectively. The O_2RhCO and ORhCO^- molecules have also been observed in the rare-gas matrixes. Previous argon matrix investigations of the reactions of laser-ablated Co metal atoms with CO_2 molecules have characterized the OC_2CO , OC_2CO^- , and CoCO_2^- molecules.²³ Present neon experiments produce new absorptions of the O_2CoCO , OC_2CO , and OC_2CO^+ molecules. Density functional theory calculations have been performed on these products, which support the experimental assignments of the infrared spectra.

Acknowledgment. The authors would like to express thanks to the reviewers for valuable suggestions. We gratefully acknowledge financial support for this research by a Grant-in-Aid for Scientific Research (B) (Grant 17350012) from the Ministry of Education, Culture, Sports, Science and Technology (MEXT) of Japan. L.J. thanks MEXT of Japan and Kobe University for an Honors Scholarship.

References and Notes

- Palmer, D. A.; van Eldik, R. *Chem. Rev.* **1983**, *83*, 651.
- Culter, A. R.; Hanna, P. K.; Vites, J. C. *Chem. Rev.* **1988**, *88*, 1363.
- Jessop, P. G.; Ikariya, T.; Noyori, R. *Chem. Rev.* **1995**, *95*, 259.
- Freund, H. J.; Roberts, M. W. *Surf. Sci. Rep.* **1996**, *25*, 225.
- Gibson, D. H. *Chem. Rev.* **1996**, *96*, 2063.
- Gibson, D. H. *Coord. Chem. Rev.* **1999**, *185–186*, 335.
- Solymosi, F. *J. Mol. Catal.* **1991**, *65*, 337.
- Creutz, C. In *Electrochemical and Electrocatalytic Reactions of Carbon Dioxide*; Sullivan, B. P., Krist, K., Guard, H. E., Eds.; Elsevier: Amsterdam, 1993.
- Erdohelyi, A.; Cserenyi, J.; Solymosi, F. *J. Catal.* **1993**, *144*, 287.
- Chen, Y. G.; Tomishige, K.; Yokoyama, K.; Fujimoto, K. *Appl. Catal., A* **1997**, *165*, 335.
- Kafafi, Z. H.; Hauge, R. H.; Billups, W. E.; Margrave, J. L. *J. Am. Chem. Soc.* **1983**, *105*, 3886 (Li + CO_2).
- Kafafi, Z. H.; Hauge, R. H.; Billups, W. E.; Margrave, J. L. *Inorg. Chem.* **1984**, *23*, 177 (Cs + CO_2).
- Andrews, L.; Tague, T. J., Jr. *J. Am. Chem. Soc.* **1998**, *120*, 13230 (Be + CO_2).
- Solov'ev, V. N.; Polikarpov, E. V.; Nemukhin, A. V.; Sergeev, G. B. *J. Phys. Chem. A* **1999**, *103*, 6721 (Mg + CO_2).
- Zhou, M. F.; Andrews, L. *J. Am. Chem. Soc.* **1998**, *120*, 13230 (Sc, Y + CO_2).
- Mascetti, J.; Tranquille, M. *J. Phys. Chem.* **1988**, *92*, 2177; *Coord. Chem. Rev.* **1999**, *190–192*, 557 (Ti, V, Cr, Fe, Co, Ni, Cu + CO_2).
- Chertihin, G. V.; Andrews, L. *J. Am. Chem. Soc.* **1995**, *117*, 1595 (Ti + CO_2).
- Zhou, M. F.; Andrews, L. *J. Phys. Chem. A* **1999**, *103*, 2066 (Ti, V + CO_2).
- Zhang, L.; Wang, X.; Chen, M.; Qin, Q. *Z. Chem. Phys.* **2000**, *254*, 231 (Zr + CO_2).
- Chen, M.; Wang, X.; Zhang, L.; Qin, Q. *Z. J. Phys. Chem. A* **2000**, *104*, 7010 (Nb + CO_2).
- Wang, X.; Chen, M.; Zhang, L.; Qin, Q. *Z. J. Phys. Chem. A* **2000**, *104*, 758 (Ta + CO_2).
- Souter, P. F.; Andrews, L. *Chem. Commun.* **1997**, 777; *J. Am. Chem. Soc.* **1997**, *119*, 7350 (Cr, Mo, W + CO_2).
- Zhou, M. F.; Liang, B.; Andrews, L. *J. Phys. Chem. A* **1999**, *103*, 2013 (Cr–Zn + CO_2).
- Liang, B.; Andrews, L. *J. Phys. Chem. A* **2002**, *106*, 595 (Re + CO_2).
- Liang, B.; Andrews, L. *J. Phys. Chem. A* **2002**, *106*, 4042 (Os, Ru + CO_2).
- Andrews, L.; Zhou, M. F.; Liang, B.; Li, J.; Bursten, B. E. *J. Am. Chem. Soc.* **2000**, *122*, 11440 (U, Th + CO_2).
- Bulkholder, T. R.; Andrews, L.; Bartlett, R. J. *J. Phys. Chem.* **1993**, *97*, 3500 (B + CO_2).
- Quere, A. M. L.; Xu, C.; Manceron, L. *J. Phys. Chem.* **1991**, *95*, 3031 (Al + CO_2).
- Brock, L. R.; Duncan, M. A. *J. Phys. Chem.* **1991**, *95*, 3031 (Al + CO_2).
- Howard, J. A.; McCague, C.; Sutcliffe, R.; Tse, J. S.; Joly, H. A. *J. Chem. Soc., Faraday Trans.* **1995**, *91*, 799 (Al, Ga + CO_2).
- Himmel, H. J.; Downs, A. J.; Greene, T. M. *Chem. Rev.* **2002**, *102*, 4191, and references therein.

- (32) Papai, I.; Mascetti, J.; Fournier, R. *J. Phys. Chem. A* **1997**, *101*, 4465.
- (33) Fan, H. J.; Liu, C. W. *Chem. Phys. Lett.* **1999**, *300*, 351.
- (34) Sodupe, M.; Branchadell, V.; Rosi, M.; Bauschlicher, C. W., Jr. *J. Phys. Chem. A* **1997**, *101*, 7854.
- (35) See, for example: Xu, C.; Manceron, L.; Perchard, J. P. *J. Chem. Soc., Faraday Trans.* **1993**, *89*, 1291. Bondybey, V. E.; Smith, A. M.; Agreiter, J. *Chem. Rev.* **1996**, *96*, 2113. Fedrigo, S.; Haslett, T. L.; Moskovits, M. *J. Am. Chem. Soc.* **1996**, *118*, 5083. Khriachtchev, L.; Pettersson, M.; Runeberg, N.; Lundell, J.; Rasanen, M. *Nature* **2000**, *406*, 874. Himmel, H. J.; Manceron, L.; Downs, A. J.; Pullumbi, P. *J. Am. Chem. Soc.* **2002**, *124*, 4448. Li, J.; Bursten, B. E.; Liang, B.; Andrews, L. *Science* **2002**, *295*, 2242. Andrews, L.; Wang, X. *Science* **2003**, *299*, 2049.
- (36) Zhou, M. F.; Tsumori, N.; Li, Z.; Fan, K.; Andrews, L.; Xu, Q. *J. Am. Chem. Soc.* **2002**, *124*, 12936. Zhou, M. F.; Xu, Q.; Wang, Z.; von Ragué Schleyer, P. *J. Am. Chem. Soc.* **2002**, *124*, 14854. Jiang, L.; Xu, Q. *J. Am. Chem. Soc.* **2005**, *127*, 42. Xu, Q.; Jiang, L.; Tsumori, N. *Angew. Chem., Int. Ed.* **2005**, *44*, 4338. Jiang, L.; Xu, Q. *J. Am. Chem. Soc.* **2005**, *127*, 8906.
- (37) Burkholder, T. R.; Andrews, L. *J. Chem. Phys.* **1991**, *95*, 8697.
- (38) Zhou, M. F.; Tsumori, N.; Andrews, L.; Xu, Q. *J. Phys. Chem. A* **2003**, *107*, 2458. Jiang, L.; Xu, Q. *J. Chem. Phys.* **2005**, *122*, 034505.
- (39) Frisch, M. J.; Trucks, G. W.; Schlegel, H. B.; Scuseria, G. E.; Robb, M. A.; Cheeseman, J. R.; Montgomery, J. A., Jr.; Vreven, T.; Kudin, K. N.; Burant, J. C.; Millam, J. M.; Iyengar, S. S.; Tomasi, J.; Barone, V.; Mennucci, B.; Cossi, M.; Scalmani, G.; Rega, N.; Petersson, G. A.; Nakatsuji, H.; Hada, M.; Ehara, M.; Toyota, K.; Fukuda, R.; Hasegawa, J.; Ishida, M.; Nakajima, T.; Honda, Y.; Kitao, O.; Nakai, H.; Klene, M.; Li, X.; Knox, J. E.; Hratchian, H. P.; Cross, J. B.; Adamo, C.; Jaramillo, J.; Gomperts, R.; Stratmann, R. E.; Yazyev, O.; Austin, A. J.; Cammi, R.; Pomelli, C.; Ochterski, J. W.; Ayala, P. Y.; Morokuma, K.; Voth, G. A.; Salvador, P.; Dannenberg, J. J.; Zakrzewski, V. G.; Dapprich, S.; Daniels, A. D.; Strain, M. C.; Farkas, O.; Malick, D. K.; Rabuck, A. D.; Raghavachari, K.; Foresman, J. B.; Ortiz, J. V.; Cui, Q.; Baboul, A. G.; Clifford, S.; Cioslowski, J.; Stefanov, B. B.; Liu, G.; Liashenko, A.; Piskorz, P.; Komaromi, I.; Martin, R. L.; Fox, D. J.; Keith, T.; Al-Laham, M. A.; Peng, C. Y.; Nanayakkara, A.; Challacombe, M.; Gill, P. M. W.; Johnson, B.; Chen, W.; Wong, M. W.; Gonzalez, C.; Pople, J. A. *Gaussian 03*, revision B.04; Gaussian, Inc.: Pittsburgh, PA, 2003.
- (40) Becke, A. D. *Phys. Rev. A* **1988**, *38*, 3098. Perdew, J. P. *Phys. Rev. B* **1986**, *33*, 8822.
- (41) McLean, A. D.; Chandler, G. S. *J. Chem. Phys.* **1980**, *72*, 5639. Krishnan, R.; Binkley, J. S.; Seeger, R.; Pople, J. A. *J. Chem. Phys.* **1980**, *72*, 5650.
- (42) Hay, P. J.; Wadt, W. R. *J. Chem. Phys.* **1985**, *82*, 299.
- (43) Citra, A.; Andrews, L. *J. Phys. Chem. A* **1999**, *103*, 4845 (Rh + O₂).
- (44) Chertihin, G. V.; Citra, A.; Andrews, L.; Bauschlicher, C. W., Jr. *J. Phys. Chem. A* **1997**, *101*, 8793 (Co + O₂).
- (45) Jacox, M. E.; Milligan, D. E. *J. Chem. Phys.* **1971**, *54*, 3935.
- (46) Jacox, M. E.; Thompson, W. E. *J. Chem. Phys.* **1989**, *91*, 1410.
- (47) Zhou, M. F.; Andrews, L. *J. Chem. Phys.* **1999**, *110*, 2414.
- (48) Zhou, M. F.; Andrews, L. *J. Chem. Phys.* **1999**, *110*, 6820.
- (49) Zhou, M. F.; Zhang, L. N.; Chen, M. H.; Qin, Q. *Z. J. Chem. Phys.* **2000**, *112*, 7089.
- (50) Darling, J. H.; Ogden, J. S. *J. Chem. Soc., Dalton Trans.* **1972**, 2496.
- (51) Zhou, M. F.; Andrews, L.; Bauschlicher, C. W., Jr. *Chem. Rev.* **2001**, *101*, 1931.
- (52) Tremblay, B.; Manceron, L.; Gutsev, G.; Andrews, L.; Partridge, H., III. *J. Chem. Phys.* **2002**, *117*, 8479.
- (53) See, for example: Mebel, A. M.; Hwang, D. Y. *J. Phys. Chem. A* **2000**, *104*, 11662. Hwang, D. Y.; Mebel, A. M. *J. Chem. Phys.* **2002**, *116*, 5633.